Title

Toxicological Profiling of Highly Purified Single-Walled Carbon Nanotubes with Different Lengths in the Rodent Lung and Escherichia Coli

Journal

Small, 14(23)

ISSN

1613-6810

Authors

Wang, Xiang
Lee, Jae-Hyeok
Li, Ruibin
et al.

Publication Date

2018-06-01

DOI

10.1002/smll.201703915

Peer reviewed

HHS Public Access

Author manuscript

Small. Author manuscript; available in PMC 2019 June 01.

Published in final edited form as:

Small. 2018 June ; 14(23): e1703915. doi:10.1002/smll.201703915.

Toxicological Profiling of Highly-Purified Single-Walled Carbon Nanotubes with Different Lengths in the Rodent Lung and *E. coli*

Xiang Wang[#†,‡], **Jae-Hyeok Lee**[##,α], **Ruibin Li**[†], **Yu-Pei Liao**[†], **Joohoon Kang**[#], **Chong Hyun Chang**[‡], **Linda M. Guiney**[#], **Vahid Mirshafiee**[‡], **Linjiang Li**[‡], **Jianqin Lu**[†], **Tian Xia**[†,‡], **Mark C. Hersam**[#,ζ], and **André E. Nel**[†,‡,*]

[†] Division of NanoMedicine, Department of Medicine, University of California, Los Angeles, CA 90095, United States

[‡] California NanoSystems Institute, University of California, Los Angeles, CA 90095, United States

[#] Department of Materials Science and Engineering, Northwestern University, Evanston, Illinois 60208, United States

[ζ] Departments of Chemistry, and Medicine, Northwestern University, Evanston, Illinois 60208, United States

[α] Predictive Model Research Center, Korea Institute of Toxicology (KIT), Daejeon 34114, Republic of Korea

[#] These authors contributed equally to this work.

Abstract

Carbon nanotubes (CNTs) exhibit a number of physicochemical properties that contribute to adverse biological outcomes. However, it is difficult to define the independent contribution of individual properties without purified materials. We prepared a library of highly purified SWCNTs of different lengths from the same base material by density gradient ultracentrifugation, designated as short (318 nm), medium (789 nm), and long (1215 nm) SWCNTs. *In vitro* screening showed length-dependent IL-1β production, in order of long > medium> short. However, there were no differences in transforming growth factor (TGF-β1) production in BEAS-2B cells. Oropharyngeal aspiration showed that all the SWCNTs induced pro-fibrogenic effects in mouse lung at 21 days post-exposure but there were no differences between tube lengths. In contrast, these SWCNTs demonstrated length-dependent antibacterial effects on *E. coli*, with long SWCNT exerting stronger effects than the medium or short tubes. These effects were reduced by Pluronic F108 coating or supplementing with glucose. Our data show that length-dependent effects on pro-inflammatory response in macrophage cell line and antibacterial effects, but not on collagen deposition in the lung. These data demonstrate that over the length scale tested, the biological response to highly purified SWCNTs is dependent on the complexity of the nano/bio interface.

[*]Corresponding Author: André E. Nel, M.D./Ph.D., Department of Medicine, Division of NanoMedicine, UCLA School of Medicine, 52-175 CHS, 10833 Le Conte Ave, Los Angeles, CA 90095-1680. Tel: (310) 825-6620, Fax: (310) 206-8107, anel@mednet.ucla.edu.

Competing interests

The authors declare that they have no competing interest.

Keywords

SWCNT; length sorting; density gradient ultracentrifugation (DGU); lung fibrosis; antibacterial effects

BACKGROUND

Single-walled carbon nanotubes (SWCNTs) exhibit unique physicochemical properties, including high tensile strength, a band gap varying from zero to ~2 eV, and a variety of electronic phenomena that can be used for sensors, electronics, batteries and integrated circuits.[1–3] The increased commercial use of SWCNTs also enhances the possibility of human exposure during the manufacturing and processing of materials that contain SWCNTs.[4] For instance, the aerosolization of SWCNT powders could lead to inhalation exposure in humans. Moreover, SWCNTs have been demonstrated to induce acute and chronic inflammation in the lungs of experimental animals, including the ability to induce pro-fibrogenic effects.[5–7] It is interesting that most toxicological studies on SWCNTs to date have focused on as-synthesized materials that generally consist of a mixture of nanotube properties which could include length, chirality, metallic vs. semiconductor properties, levels of surface defects or different types of surface functionalization. As a result, it is difficult to ascribe the contribution of individual nanotube properties to specific adverse outcomes. Although attempts have been made to obtain highly purified SWCNTs for establishing property-activity relationships, this is a challenging undertaking. While it is generally accepted that long and stiff (micron scale) CNTs are more toxic than shorter or tangled tubes (nano-micron scale) tubes, the data are based on materials of heterogeneous composition, without attempts to purify tubes of the same length or develop a tube-length series that is based on the same starting material.[8–13] Moreover, although it has been shown that tubes longer than 10 μm could act like fibers, with the ability to induce frustrated phagocytosis, [11, 14–17] our own studies have shown that SWCNTs and MWCNTs at length scales well below those that frustrated phagocytosis, can induce acute and chronic lung injury.[6, 7, 18–21]

In order to investigate the hazard potential of length-sorted SWCNTs that are derived from the same starting material, we developed a density gradient ultracentrifugation (DGU) method for SWCNT purification.[22, 23] DGU allows fractionation of polydisperse SWCNTs into finely-sorted materials that can be separated according to tube length or electronic properties (e.g., metallic or semiconductor). This purification method also yields sufficient tube quantities for performance of structure-activity analysis, which allows one to address the role of individual tube properties to biological outcome.[20, 22] One of our preferred study approaches to assessing SWCNT and MWCNT properties is to study their pro-fibrogenic effects pulmonary cell types and the lung.[6, 7, 18–21, 24, 25] Many of these studies have demonstrated that the long aspect ratio of these materials, rather than fiber-like dimensions, play a role in triggering lysosomal damage and IL-1β release in macrophages, which synergize with the ability of these materials to induce TGF-β1 production in lung epithelial cells.[6, 7, 18–21, 24, 25] Collectively, these processes are involved in epithelial-

mesenchymal transition (EMT), culminating in chronic inflammation and collagen deposition in the lung.[26]

In this study, we made use of DGU fractionation to prepare a series of highly purified SWCNTs of different length (from the same starting material) to investigate the impact on pro-fibrogenic effects in the lung. In addition, we also assessed CNT length effects in *E. coli*, where it has been shown that SWCNTs are capable of inducing contact-dependent membrane damaging effects.[27, 28] In addition to the starting as-purchased material, we obtained a series of SWCNTs with average lengths of 318 (short), 789 (medium) and 1215 nm (long). While the differences in tube length did not alter their pro-fibrogenic effects in the lung, there was a differential effect on damaging lysosomes and inducing IL-1β production in macrophages. We also observed length-dependent effects on *E Coli* growth, with long tubes capable of inducing more severe, contact-dependent membrane effects. Collectively, these data demonstrate that while SWCNTs can result in length-dependent effects under some exposure scenarios, the complexity of the nano/bio interface may determine to what extent tube length influence the outcome.

RESULTS

Fractionation, purification and characterization of different length SWCNTs

We used density gradient ultracentrifugation (DGU) to separate SWCNT populations of varying length scale, as described in Materials and Methods. Figure 1A provides a schematic illustration and pictures of the fractionated SWCNT solutions during DGU sedimentation. Briefly, the process begins by sonicating as-synthesized SWCNTs at 9 W or 40 W for 2 hours in a surfactant solution, containing 2% w/v sodium deoxycholate (SDC). This suspension is centrifuged to remove aggregated SWCNTs, yielding a surfactant solution containing individually separated SWCNTs. Subsequently, the SWCNT dispersion is subjected to DGU sedimentation in an iodixanol density gradient. DGU fractionation yielded three major SWCNT populations that differ by length, as confirmed by atomic force microscopy (AFM) and optical absorbance spectroscopy. Figure 1B shows the length versus diameter histograms, demonstrating average length scales of 318, 789 and 1215 nm, at a consistent diameter. We labeled the length-sorted SWCNT fractions as short, medium and long SWCNTs, respectively. Their representative AFM images are shown in Figure 1C, and demonstrate the presence of individualized tubes with minimal aggregation and average diameter size of ~0.86 nm. The corresponding AFM histograms of unsorted SWCNTs are provided in Figure S1, which shows a larger length distribution as expected. Figure 1D provides optical absorbance spectra of the three length-sorted SWCNTs fractions. The two primary peaks at ~566 nm and ~976 nm are characteristic of the semiconducting (6,5) CoMoCAT SWCNTs used in this study.

ICP-MS was employed to identity and quantify residual catalysts in the tube samples (Table 1). The level of Co and Mo in the short SWCNTs were 4.0 wt% and 5.27 wt%, 0.70 wt% and 3.76 wt% in the medium SWCNTs, and 1.55 wt% and 4.18 wt% in the long SWCNTs, respectively. The corresponding levels of the unsorted SWCNTs were 7.80 wt% and 8.55 wt %, respectively (Table 1). Assessment of the hydrodynamic size by dynamic light scattering (HT-DLS, Dynapro Plate Reader, Wyatt Technology) showed hydrodynamic diameters of

10,124 nm, 17,712 nm, 25,002 nm, respectively, for the short, medium and long SWCNTs suspended in deionized water (DI H_2O). These hydrodynamic sizes decreased when the SWCNT samples were suspended in complete RPMI1640, BEGM, and LB medium (Table 2) as a consequence of the coating of the tube surfaces by proteins. The zeta potentials of the SWCNTs ranged from −9.9 to −17.3 mV in DI H_2O and −6.8 to −14.6 mV in cell culture media (Table 2).

The effect of SWCNT length scale on cytotoxicity and pro-inflammatory effects in tissue culture cells

We tested the cytotoxic potential and pro-inflammatory effects of sorted SWCNTs in THP-1 and BEAS-2B cell lines. THP-1 cells were chosen for their ability to differentiate into macrophage-like cells, which are capable of assembling NLRP3 inflammasome components in response to long aspect ratio materials (such as CNTs) or rare earth oxides. BEAS-2B is a human bronchial epithelial cell line that responds to CNTs with TGF-β1 production. Both represent portal-of-entry cell types that may encounter nanoparticles in the lung. We used an MTS assay to demonstrate that the sorted SWCNTs have minor effects on THP-1 viability at lower doses (12.5 and 25 μg/mL) but induced more than a 40% decrease in viability at the highest dose for short and medium SWCNTs. However, there was no statistically significant difference between the tubes at the highest dose level (Figure 2A). In the case of BEAS-2B cells, only the short tubes exerted statistically significant reduction in viability at the highest dose of 100 μg/mL (Figure 2B). In contrast, there was a significant decrease in cell viability in response to nano-ZnO, used as a positive control. These results also agree with an ATP assay, which demonstrated modest length-dependent effects on the viability of both cell types (Figure S2A and B).

IL-1β production and release into the supernatants of THP-1 cells was assessed to determine if tube length has an effect on NLRP3 inflammasome activation. The results demonstrate a length-dependent increase in IL-1β production in the order, long > medium > short tubes (Figure 2C). Unsorted tubes also induced IL-1β production that was approximately of similar magnitude as of those medium-length tubes. Monosodium urate (MSU), which was used as the positive control, induced the most robust response (Figure 2C). We also used BEAS-2B cells to assess the production of TGF-β1, which acts as a pro-fibrogenic growth factor in the lungs of SWCNT-exposed animals.[6, 20] In spite of the fact that TGF-β1 production by the epithelial cells was less robust than IL-1β release from THP-1 cells, there was no differences in the responses of both length-sorted or unsorted SWCNTs (Figure 2D). IL-1β and TGF-β1 exert synergistic effects during the induction of epithelial-mesenchymal transition (EMT) in the intact animal lung.[7, 21, 26]

Since direct cellular contact or uptake is required for the responses depicted in Figure 2, we compared the relative abundance of cellular association with sorted and unsorted tubes by side scatter analysis (flow cytometry) in THP-1 cells. No differences were observed for tubes of different lengths size (Figure S3). This suggested that the differences in IL-1β production result could be determined by the intracellular fate of the materials, including effects on the lysosomes. A fluorescent cathepsin B substrate, Magic Red, was used to assess lysosome integrity and enzyme release by confocal microscopy (Figure 2E).

Compared to the punctate distribution of cathepsin B in intact lysosomes in untreated cells, damage to this organelle by MSU or unsorted tubes leads to cytosolic release and diffuse intracellular spread of the dye. We also observed that sorted tubes can induce size - dependent damage to the lysosomal membrane, with long tubes releasing more Magic Red than medium and short tubes (Figure 2E). These results are consistent with the induction of IL-1β release from THP-1 cells (Figure 2C). All considered, the confocal data reveals length-dependent SWCNT effects in THP-1 cells.

SWCNTs induce pro-fibrogenic effects in the lung, irrespective of length.

We have previously demonstrated that the aspect ratio, state of dispersion, hydrophobicity, metal impurities, surface reactivity, and chirality contribute to the hazardous pulmonary effects of CNTs.[6, 7, 18, 20, 21, 29–31] These properties affect cellular uptake, lysosomal localization, catalytic injury to the lysosome membrane, assembly of the NLRP3 inflammasome and IL-1β production in pulmonary macrophages. The activation of the macrophages contributes to the EMT process, during which the production of pro-fibrogenic growth factors (e.g., TGF-β1 and PDGF-AA) by epithelial cells lead to collagen deposition in the lung.[7, 26] To determine to what extent SWCNT length may impact pro-fibrogenic effects in the lung, oropharyngeal aspiration of the length-sorted SWCNTs was performed in C57BL/6 mice. We selected an exposure dose that is based on the occupational assessment of airborne CNT levels in a production facility, where ambient exposure levels can attain levels as high as 400 $\mu g/m^3$. Using this as the theoretical exposure amount in an adult subject breathing ambient air at 10 L/min and assuming a 30% deposition rate for the tubes during an occupational exposure for 32 weeks (8 h/day, 5 d/week), the total lung burden will be 92.16 mg. Assuming an alveolar surface area of 102 m^2 in a human adult, the equivalent surface area dose amounts to 903.53 $\mu g/m^2$ in the lung of an exposed human worker. This equals 1.81 mg/kg in a 25 g mouse with an alveolar epithelial surface area of 0.05 m^2. In accordance with these calculations, we selected a bolus instillation dose of 2 mg/kg for sorted and unsorted SWCNTs in mice. The positive control was 5 mg/kg Min-U-Sil (α-quartz), a highly reactive material that causes chronic lung inflammation and fibrosis.

Previous studies from our laboratory showed that IL-1β production in the lung is an early event (in the first few days), which sets in motion the march of events that subsequently leads to EMT and production of pro-fibrogenic growth factors.[7, 21] We therefore assessed IL-1β levels in the bronchoalveolar lavage fluid (BALF) 40 h after oropharyngeal aspiration. While the results showed that all the sorted and unsorted SWCNTs could induce IL-1β production, there was no length-dependent effect (Figure S4). This is similar to the data on pro-fibrogenic growth factors in the BALF. Thus, the in vitro differences of IL-1β production were negated by a more complex nano/bio interface at the organ level.

Another animal sacrifice was performed 21 days after exposure. Examination of the BALF demonstrated non-significant changes in the total and differential cell counts in response to the various SWCNTs preparations. Histological examination showed mild pulmonary inflammation in response to quartz and all SWCNT preparations (not shown). These morphological changes were accompanied by significant increases in TGF-β1 and PDGF-AA levels in the BALF of quartz and all SWCNT exposed animals (Figure 3A and B).

Although quartz induced the biggest response, there were no differences in TGF-β1 or PDGF-AA levels between the different tube types. These results agree with the measurement of collagen deposition in the lung, determined by a Sircol assay. This demonstrated approximately similar increases in the collagen content in lung tissue during exposure to quartz, non-sorted and length-sorted SWCNTs (Figure 3C). Moreover, standing of the lung tissue by Masson's trichrome, revealed approximately the same limited amount of collagen deposition in response to sorted and unsorted SWCNTs (Figure 3D). These results indicate that, in spite of differences in IL-1β production in THP-1 cells, it was not possible to demonstrate a length-dependent effect of SWCNTs on collagen deposition in the lung. A possible reason for the differences in vitro and in vivo is that compared to the tissue culture (THP-1 cell) conditions, the heterogeneous cellular population in the lung do not have the discriminatory ability of a single cell type to discern tube length differences during the generation of the EMT process.

Length-dependent antibacterial effects in *E. coli*.

In addition to the hazard potential in a mammalian organ, such as the lung, SWCNTs also pose a danger to the environment, including exerting anti-bacterial effects in a model organism like *E. coli*. [27, 28, 32–40] Putatively, these damaging effects are caused by direct tube interactions with the bacterial membrane.[27, 28, 32] While we have been able to use DGU-purified metallic and semiconductor SWCNTs to study their effects in *E. coli*, similar investigations for length-sorted tubes have not been carried out.[20] Utilizing length-sorted tubes, we looked at the effect on bacterial growth in LB media. We inoculated *E. coli* cultures in log-phase growth with 12.5–200 μg/mL of the length-sorted tubes, and determine cell densities (OD_{600}) after 24 hours. The results demonstrated a differential effect on E. *coli* growth inhibition in the hierarchical order long > medium > short tubes (Figure 4A). Unsorted SWCNTs had approximately the same growth inhibitory effects as medium length tubes (Figure 4A). Moreover, we also compared the growth inhibitory effects to the morphology of the bacteria, using scanning electron microscopy (SEM) (Figure 4B). This demonstrated that the uniform rod-shaped appearance and smooth surface of the bacteria undergoing changes during incubation with medium and long tubes. Not only did the nanotubes adhere to the bacterial surfaces, but they induced incremental sharpening of the cell and membrane ruffling. Small tubes had little effect, while unsorted SWCNTs had approximately the same effect as long tubes.

The tight adherence of medium, long and unsorted tubes to the bacterial surface suggests a membrane damaging effect, as previously reported for SWCNTs.[27, 32, 41] This notion was confirmed by coating the sorted tubes with the block copolymer, Pluronic F108 (PF108), which leads to the formation of a brush-like coating on the tube surface. Pluronic coating improves the suspension stability of the nanotubes in aqueous media and also interferes in direct tube binding to the surface membrane.[21, 42] It is therefore of interest that PF108 coating could reverse the growth inhibitory effects of long, medium and unsorted tubes in *E. coli* (Figure 5A-D). PF108 coating also improved the in the morphological damage in response to long tubes (Figure 5E). It was also possible to improve the growth inhibitory effects of medium and long tubes through the use of glucose to supplement the bacterial growth medium (Figure S5). SEM confirmed the improvement in bacterial morphology

under these growth conditions (data not shown). In summary, the bacterial data demonstrate clear evidence of length-dependent bactericidal effects for SWCNTs.

DISCUSSION

In this study, we assessed the biological impact of highly purified SWCNTs at different length scales in mammalian cells, bacteria and the murine lung. *In vitro* screening showed length-dependent induction of IL-1β production by the SWCNTs in THP-1 cells, with the longer tubes being more toxic. However, there were no length-dependent differences in TGF-β1 production in an epithelial cell line, which also agrees with the lack of differential effect in the induction of increased collagen deposition in the lung. Length-sorted nanotubes also did not show differences from the base material in terms of their pro-fibrogenic effect in the lung. However, similar to the effect of macrophages, long tubes inducing significantly higher antibacterial effects in *E. coli* than medium length tubes, while short tubes had no effect. The antibacterial effects of the longer tubes were dependent on tube adherence to the bacterial membrane, leading to morphological changes that are reversible by PF108 coating or supplementation of the bacterial growth medium with glucose. All considered, these data demonstrate that over the length scale 318–1250 nm, SWCNTs could generate adverse biological effects, the outcome of which is dependent on the complexity of the environment in which the exposure occurs.

One of the important findings of this study is that CNTs can induce pro-fibrogenic effects at the submicron length scale, which indicates that the pulmonary hazard potential is not restricted to fiber -like dimensions only.[11, 12, 16, 17, 43] Many of the toxicological studies premised on the fiber paradigm have made use of MWCNTs, such as Mitsui-7, with length scales up to 10 μm or more in comparison to shorter tubes.[8–10, 12, 13, 28, 40] Not only did the acquired materials include a heterogeneous mixture of length scales, but involved comparisons to shorter tubes of different physical chemical composition, and hence, including property variations other than length. Attempts to improve the analysis with purified materials have been challenging without suitable separation techniques for sorting tube length, as well as transferring purified materials into biologically appropriate buffers. Our study demonstrates the use of a DGU separation technique that allowed us to prepare length-sorted SWCNTs from the same starting material, in addition to allowing material preparation in biologically relevant aqueous media. Strikingly, this allowed us to demonstrate a length-dependent effect on IL-1β production, premised on the molecular initiating event that involve lysosomal damage by long and medium length tubes (Figure 2E). The CNTs were dispersed by BSA and DPPC, using a widely used NIOSH protocol.[44–46] While BSA plus DPPC have been shown to contribute to the formation of a corona on the CNT surface, we do not have any reason to believe that the effect selectively changed the bioreactivity of individual materials in the library.[44–46] We do not know for sure what the mechanism is for the length-dependent effects of CNTs in lysosome damage. What we do know is that longer tubes have higher hydrodynamic sizes than short ones, which means that in any enclosed space after phagocytosis, there is an increased chance of interacting with the phagolysosomal membrane. This opens up the possibility that additional physicochemical features such as a reactive tube surface or the generation of oxygen radicals may lead to membrane damage.[47–50] Thus, a combination of tube length, aspect ratio and surface

reactivity may determine the site of intracellular localization and catalytic damage to the particular endosomal compartments. However, this effect is limited to phagocytic cell types like macrophages, which differs from the response in epithelial cells, which requires activation of the TGF-β/SMAD pathway.[51, 52] Since the epithelial response may not be critically length-dependent, this could explain why the intermingling of the macrophage with the epithelial cell responses *in vivo* may not result in increased collagen deposition in the lung.

In contrast to our observations in the mammalian system, several studies have demonstrated that a SWCNTs suspensions or composite films can exert antibacterial effects.[27, 28, 32–40] This includes the demonstration that longer length (>5 μm) SWCNTs in E. coli exhibit more robust antimicrobial activity than shorter (<1 μm) tubes.[28] Moreover, our own study demonstrates that medium, long and unsorted SWCNTs form a meshwork that is tightly adherent to the *E. coli* membrane, while short tubes fail to do so (Figure 4B). It is possible that this interaction leads to lipid peroxidation in the bacterial membrane, leading to interference in bacterial growth and morphological changes. The importance of adhesion to the bacterial membrane was confirmed by coating long SWCNTs with the triblock copolymer, PF108, which adheres to the SWCNT surface through its intermediary hydrophobic segment, allowing the hydrophilic blocks to form brush-like protrusions that provide steric hindrance.[21, 42] PF108 coating interfered in the growth inhibitory effects of long, medium and unsorted SWCNTs. Interestingly, the growth inhibitory effects of uncoated tubes could also be reversed by supplementing the LB medium with glucose (Figure S5). The same phenomenon has also been observed with other SWCNTs and 2-dimensional nanomaterials, such as graphene and graphene oxide.[40, 53–55]

Our study is important for understanding the structure-activity relationships (SAR) that underpin SWCNT toxicity. Although SAR studies have shown that a number of physicochemical properties may contribute to CNT toxicity *in vitro* and *in vivo*, there are knowledge gaps about the exact role of CNT properties such as tube length. Our ability to use DGU to prepare highly pure, length-sorted tubes demonstrates its value for performing biological structure-activity analysis. Similarly, there is also an increasing trend in using highly purified SWCNTs for electronic and non-biological applications, it is also important to adapt these methods to allow safety investigations. Through our use of the DGU method in conjunction with *in vitro* and *in vivo* assessment strategies, we have been able to show how length-sorted SWCNTs can be introduced for predictive toxicological assessment of an important parameter in a similar way as recently undertaken for the study of semiconductor versus metallic properties of SWCNTs.[6, 20] We have also used the establishment of nanomaterial libraries to study the SARs of other carbonaceous nanomaterials, including graphene and graphene oxide.[6, 56] The current study demonstrates that in addition to using the approach for assessment of pulmonary toxicity, the sorted SWCNTs can also be used to study antibacterial effects in E. coli.

CONCLUSION

In summary, through the use of highly purified, length-sorted SWCNTs, we demonstrate that it is indeed possible to discern differences in the biological behavior of SWCNTs over a

length scale of 318–1215 nm. However, while we observed differences in macrophage injury responses, no length dependent pro-fibrogenic effects were observed in epithelial cells and the lung. We did observe, however, that longer tubes could damage the E. coli membrane, leading to growth inhibitory effects. These effects could be alleviated by surface coating with a polymer or adding glucose to the bacterial growth meeting.

MATERIALS AND METHODS

Preparation of length-sorted SWCNT solutions:

Length-sorted single-walled carbon nanotubes (SWCNTs) were prepared by sedimentation density gradient ultracentrifugation (DGU), following a previously described method.[22, 23] To minimize the diameter range of the tubes, (6,5) enriched CoMoCAT-synthesized SWCNTs (Southwest NanoTechnologies Inc., SG65i, purity ≥95%) were used as the starting material. In a typical procedure, 20 mg of CoMoCAT SWCNTs were dispersed in an aqueous solution of 2 % w/v sodium deoxycholate (SDC, Sigma Aldrich) using a horn tip sonicator (Fisher Scientific, Sonic Dismembrator 500) at 9 W or 40 W power for 2 hours, followed by centrifugation to remove aggregated SWCNTs. Subsequently, OptiPrep (60% w/v iodixanol) was diluted with 2% w/v SDC solution to prepare gradient solutions for fractionation. SWCNT length separation was performed using a three-layer density gradient based on 25%, 30%, and 40% w/v iodixanol solutions, in 8 mL, 2 mL and 1.5 mL volumes, respectively. The density gradients were created in 15 mL centrifuge tubes by layered addition to provide incremental density. 2 mL of the SWCNT solution containing 30% w/v iodixanol was placed in the middle of the centrifuge tube, above the 40% iodixanol solution. Ultracentrifugation was performed for 20 hours at ~70,000 g in a SW32 Ti rotor (Optima L-80 XP, Beckman Coulter) to provide differential sedimentation as a function of SWCNT length. Fractionation was performed in 4.7 mm steps using a piston gradient fractionator (Biocomp Instruments, Inc.).

Preparation for SWCNT characterization:

The CoMoCAT SWCNTs used in this study were synthesized by a supported catalytic chemical vapor deposition (CVD) process that involves the use of cobalt (Co) and molybdenum (Mo) as catalysts. The length-sorted SWCNTs were characterized using atomic force microscopy (AFM). AFM samples were acquired by dropcasting 50 μL of SWCNT solution onto amine-modified (3-aminopropyltriethoxysilane, APTES) SiO_2 substrates. After 15 seconds, the substrate was gently rinsed with deionized (DI) water, dried with N_2, and imaged by tapping mode AFM. At least 100 individual SWCNTs were measured to obtain histograms for length and diameter. Inductively coupled plasma mass spectrometry (ICP-MS) was used to determine the identity and the amount of residual catalysts in each length-sorted SWCNT sample. UV−Vis-NIR spectrometry was carried out on a Varian Cary 5000 spectrophotometer (Agilent Technologies) using a 10 mm path length microcuvette.

Preparation of sorted SWCNT Suspensions for Use in Tissue Culture:

For cytotoxicity studies, the residual chemicals (e.g., SDC and iodixanol) were removed by flocculating the SWCNTs through the addition of four volumetric parts of ethanol to one

part of tube solution. The solution was vacuum-filtered using a 0.05 μm alumina membrane (Whatman® Anodisc) and washed three times with deionized (DI) water. Following vacuum filtration, the surfactant-free SWCNTs were weighed and resuspended in DI water.

Cellular exposure to SWCNTs for assessing Cytotoxicity and Pro-Inflammatory Effects:

The SWCNT stock suspensions were prepared in DI H_2O at 1 mg/mL. BEAS-2B and THP-1 cells were obtained from ATCC (Manassas, VA). 1×10^4 BEAS-2B cells were cultured in 0.1 mL BEGM in 96-well plates at 37 °C. THP-1 cells were pretreated with 1 μg/mL phorbol 12-myristate acetate (PMA) overnight and primed with 10 ng/mL lipopolysaccharide (LPS). Aliquots of 3×10^4 primed cells were cultured in 0.1 mL medium with carbon nanotubes in 96-well plates (Costar, Corning, NY, USA) at 37 °C for 24 h. In order to provide less aggregated tubes that can be suspended in biological culture media, all SWCNT suspensions were freshly prepared by adding a desired amount of stock solutions to BEGM or RPMI 1640 media at 12.5–100 μg/mL in the presence of BSA (0.6 mg/mL) and DPPC (0.01 mg/mL). After 24 h, the supernatants were collected for the measurement of IL-1β (BD Biosciences, San Diego, CA) and TGF-β1 (Promega, Madison, WI), using ELISA kits according to manufacturer's instructions. Concentrations are expressed as pg/mL. The remaining cells were treated with 120 μL culture medium containing 16.7 % of MTS (CellTiter 96 Aqueous, Promega Corp) for 0.5 h at 37 °C. The plates were centrifuged at 2000 g for 10 min to remove the cell debris and the tubes. 85 μL of the supernatant was transferred into a new 96-well plate. The absorbance was read at 490 nm on a SpectraMax M5 microplate reader (Molecular Devices Corp., Sunnyvale, CA, USA).

Confocal Microscopy to Assess Lysosomal Damage and Cathepsin B Release:

A total of 1×10^5 primed THP-1 cells were seeded into each well of an 8-well chamber and incubated with 50 μg/mL SWCNTs for 24 h. After fixation in 4% paraformaldehyde for 1 h in PBS, cells were washed three times with PBS and stained with Magic Red (ImmunoChemistry Technologies) at 26 nM for 1 h. Following further washing in PBS, the cell nuclei were stained for 30 min with 5 μg/mL Hoechst 33342. The chamber was visualized under a confocal microscope (Leica Confocal 1P/FCS) in the CNSI Advanced Light Microscopy/Spectroscopy Shared Facility. High magnification images were obtained with the 100× objective. Untreated cells were used as control. Cells treated with 100 μg/mL monosodium urate (MSU) crystals served as the positive control.

Oropharyngeal Aspiration to assess Pulmonary Effects in Mice:

Eight-week-old male C57Bl/6 mice were purchased from Charles River Laboratories (Hollister, CA). All animals were housed under standard laboratory conditions according to UCLA guidelines for care and treatment as well as the NIH Guide for the Care and Use of Laboratory Animals in Research (DHEW78–23). The animal experiments were approved by the Chancellor's Animal Research Committee at UCLA and include standard operating procedures for animal housing (filter-topped cages; room temperature at 23 ± 2 °C; 60 % relative humidity; 12 h light, 12 h dark cycle) and hygiene status (autoclaved food and acidified water). Animal exposure was carried out according to the oropharyngeal aspiration method developed at NIOSH. The animals received oropharyngeal aspiration of short-, medium-, long-, and unsorted-SWCNTs suspended in saline at 2 mg/Kg in the presence of

BSA (0.6 mg/mL) and DPPC (0.01 mg/mL). The mice were sacrificed after 21 days to assess the sub-chronic effects. Bronchoalveolar lavage fluid (BALF) and lung tissue were collected for measurement of TGF-β1 and PDGF-AA levels and performance of Hematoxylin and Eosin (H&E) or Masson's trichrome staining.

Assessment of the effects of SWCNT Length on E. coli growth:

E. coli, strain ATCC 25922, was used to establish possible SWCNT effects on bacterial growth. Briefly, 1 mg/mL of each of the SWCNT stock solutions was dispersed in LB media at 200 μg/mL. The mixture was sonicated with a probe (Sonics & Materials, USA) for 15 s at 32, following which the suspensions were diluted in culture media in stepwise fashion to obtain two concentrations of 12.5, 25, 50, 100 and 200 μg/mL. 50 μL of each SWCNT suspension was pipetted into 384-well microplates, using 9 replicates for each dose. The log-phase bacterial culture (OD600 between 0.5~0.7) was then inoculated into the plate containing the SWCNT suspensions by a plastic 384 pin replicator (Genetix Molecular Devices). Sterility and blank controls (bacterial media with no inoculation) were included for each concentration (3 replicates). After 24 h incubation at 37 °C, a Biotek Synergy plate reader (BioTek, Winooski, VT) was used to monitor OD600. The growth curve was constructed using the following equation: $\%Growth = \frac{A_{NP,B} - A_{NP,M}}{A_B - A_{B,M}} \times 100\%$, where ANP,B is the absorbance of the bacterial culture in the presence of SWCNTs; ANP,M is the absorbance of the SWCNTs in the absence of bacteria (average of 3 replicates); AB is the absorbance of the bacterial culture in blank (no SWCNTs) media, and AB,M is the absorbance of media with no bacteria.

Scanning Electron Microscopy.

Bacteria were prepared for electron microscopy as previously described.[20] E. coli were grown in LB media to obtain a culture with an optical absorbance of 0.5–0.7 at 630 nm. One ml culture aliquots were centrifuged at 11,000×g for 10 min. The pellet was resuspended in 1 ml of a suspension containing 100 μg/mL CNTs. After incubation at 37 °C for 24 h, the suspension was centrifuged again, and the cells were washed twice with 0.1 M sodium phosphate buffer solution (PBS), pH 7.2 (PBS). Bacterial cells were fixed with 2.5% glutaraldehyde in 0.1 M PBS. Samples were postfixed with 1% (w/v) OsO_4 in 0.1 M PBS for 2 h at room temperature, washed once with the same buffer, dehydrated in a graded series of ethanol solutions, then embedded in Spurr low-viscosity embedding medium. The samples were mounted on SEM stubs and coated by PELCO SC-7 sputter for 30 sec at 30 mA to generate a thin Au/Pt conductive layer (2–20 nm). The samples were examined under a scanning electron microscope (SEM, ZEISS SUPRA 40VP).

Statistical Analysis:

Mean and standard deviations (SD) were calculated for each parameter. Results were expressed as mean ± SD of multiple determinations. Comparisons within each group were conducted by a two-sided Student's t test. A statistically significant difference was assumed with $p < 0.05$.

Supplementary Material

Refer to Web version on PubMed Central for supplementary material.

Acknowledgments

Research reported in this publication was supported by the National Institute of Environmental Health Sciences at the National Institutes of Health, under Award # RO1ES022698. Leveraged support for characterization equipment used in this study was provided by the National Science Foundation and the Environmental Protection Agency under Award No. DBI-1266377. Fluorescent microscopy was performed at the CNSI Advanced Light Microscopy/ Spectroscopy Shared Facility at UCLA. We acknowledge Nikhita D. Mansukhani, Department of Materials Science and Engineering, Northwestern University, for the advice on SWCNT preparation.

References

[1]. Geier ML, McMorrow JJ, Xu WC, Zhu J, Kim CH, Marks TJ, Hersam MC, Nat Nanotechnol 2015, 10, 944–U191. [PubMed: 26344184]

[2]. De Volder MFL, Tawfick SH, Baughman RH, Hart AJ, Science 2013, 339, 535–539. [PubMed: 23372006]

[3]. Jariwala D, Sangwan VK, Lauhon LJ, Marks TJ, Hersam MC, Chem Soc Rev 2013, 42, 2824–2860. [PubMed: 23124307]

[4]. Liu Y, Zhao YL, Sun BY, Chen CY, Accounts Chem Res 2013, 46, 702–713.

[5]. Shvedova AA, Kisin E, Murray AR, Johnson VJ, Gorelik O, Arepalli S, Hubbs AF, Mercer RR, Keohavong P, Sussman N, Jin J, Yin J, Stone S, Chen BT, Deye G, Maynard A, Castranova V, Baron PA, Kagan VE, Am J Physiol-Lung C 2008, 295, L552–L565.

[6]. Wang X, Duch MC, Mansukhani N, Ji ZX, Liao YP, Wang MY, Zhang HY, Sun BB, Chang CH, Li RB, Lin SJ, Meng H, Xia T, Hersam MC, Nel AE, ACS nano 2015, 9, 3032–3043. [PubMed: 25646681]

[7]. Wang X, Xia T, Ntim SA, Ji Z, Lin S, Meng H, Chung C, George S, Zhang H, Wang M, Li N, Yang Y, Castranova V, Mitra S, Bonner J, Nel AE, ACS nano 2011, 5 9772–9787. [PubMed: 22047207]

[8]. Brown DM, Kinloch IA, Bangert U, Windle AH, Walter DM, Walker GS, Scotchford CA, Donaldson K, Stone V, Carbon 2007, 45, 1743–1756.

[9]. Manke A, Luanpitpong S, Dong CB, Wang LY, He XQ, Battelli L, Derk R, Stueckle TA, Porter DW, Sager T, Gou HL, Dinu CZ, Wu NQ, Mercer RR, Rojanasakul Y, Int J Mol Sci 2014, 15, 7444–7461. [PubMed: 24786100]

[10]. Miozzi E, Rapisarda V, Marconi A, Costa C, Polito I, Spandidos DA, Libra M, Fenga C, Exp Ther Med 2016, 11, 21–27. [PubMed: 26889212]

[11]. Murphy FA, Poland CA, Duffin R, Donaldson K, Nanotoxicology 2013, 7, 1157–1167. [PubMed: 22812632]

[12]. Murphy FA, Schinwald A, Poland CA, Donaldson K, Particle and fibre toxicology 2012, 9.

[13]. Sweeney S, Grandolfo D, Ruenraroengsak P, Tetley TD, Int J Nanomed 2015, 10, 3115–3129.

[14]. Ryman-Rasmussen JP, Tewksbury EW, Moss OR, Cesta MF, Wong BA, Bonner JC, Am J Resp Cell Mol 2009, 40, 349–358.

[15]. Boyles MSP, Young L, Brown DM, MacCalman L, Cowie H, Moisala A, Smail F, Smith PJW, Proudfoot L, Windle AH, Stone V, Toxicology in Vitro 2015, 29, 1513–1528. [PubMed: 26086123]

[16]. Murphy FA, Poland CA, Duffin R, Al-Jamal KT, Ali-Boucetta H, Nunes A, Byrne F, Prina-Mello A, Volkov Y, Li SP, Mather SJ, Bianco A, Prato M, MacNee W, Wallace WA, Kostarelos K, Donaldson K, Am J Pathol 2011, 178, 2587–2600. [PubMed: 21641383]

[17]. Donaldson K, Murphy FA, Duffin R, Poland CA, Particle and fibre toxicology 2010, 7.

[18]. Li RB, Wang X, Ji ZX, Sun BB, Zhang HY, Chang CH, Lin SJ, Meng H, Liao YP, Wang MY, Li ZX, Hwang AA, Song TB, Xu R, Yang Y, Zink JI, Nel AE, Xia T, ACS nano 2013, 7, 2352–2368. [PubMed: 23414138]

[19]. Wang X, Liao YP, Telesca D, Chang CH, Xia T, Nel AE, Small 2017, 13.

[20]. Wang X, Mansukhani ND, Guiney LM, Lee JH, Li RB, Sun BB, Liao YP, Chang CH, Ji ZX, Xia T, Hersam MC, Nel AE, ACS nano 2016, 10, 6008–6019. [PubMed: 27159184]

[21]. Wang X, Xia T, Duch MC, Ji ZX, Zhang HY, Li RB, Sun BB, Lin SJ, Meng H, Liao YP, Wang MY, Song TB, Yang Y, Hersam MC, Nel AE, Nano Lett 2012, 12, 3050–3061. [PubMed: 22546002]

[22]. Arnold MS, Green AA, Hulvat JF, Stupp SI, Hersam MC, Nat Nanotechnol 2006, 1, 60–65. [PubMed: 18654143]

[23]. Fagan JA, Becker ML, Chun J, Hobbie EK, Adv Mater 2008, 20, 1609–1613.

[24]. Li RB, Ji ZX, Chang CH, Dunphy DR, Cai XM, Meng H, Zhang HY, Sun BB, Wang X, Dong JY, Lin SJ, Wang MY, Liao YP, Brinker CJ, Nel A, Xia T, ACS nano 2014, 8, 1771–1783. [PubMed: 24417322]

[25]. Sun B, Pokhrel S, Dunphy DR, Zhang H, Ji Z, Wang X, Wang M, Liao Y, Chang CH, Dong J, Li R, Mädler L, Brinker J, Nel A, Xia T, ACS nano 2015.

[26]. Bonner JC, Fibrogenesis & tissue repair 2010, 3, 15. [PubMed: 20738867]

[27]. Kang S, Herzberg M, Rodrigues DF, Elimelech M, Langmuir 2008, 24, 6409–6413. [PubMed: 18512881]

[28]. Yang CN, Mamouni J, Tang YA, Yang LJ, Langmuir 2010, 26, 16013–16019. [PubMed: 20849142]

[29]. Wang X, Jia G, Wang H, Nie H, Yan L, Deng XY, Wang S, J Nanosci Nanotechno 2009, 9, 3025–3033.

[30]. Wang X, Guo J, Chen T, Nie HY, Wang HF, Zang JJ, Cui XX, Jia G, Toxicology in Vitro 2012, 26, 799–806. [PubMed: 22664788]

[31]. Sun BB, Wang X, Ji ZX, Wang MY, Liao YP, Chang CH, Li RB, Zhang HY, Nel AE, Xia T, Small 2015, 11, 2087–2097. [PubMed: 25581126]

[32]. Kang S, Pinault M, Pfefferle LD, Elimelech M, Langmuir 2007, 23, 8670–8673. [PubMed: 17658863]

[33]. Kang S, Mauter MS, Elimelech M, Environ Sci Technol 2009, 43, 2648–2653. [PubMed: 19452930]

[34]. Vecitis CD, Zodrow KR, Kang S, Elimelech M, ACS nano 2010, 4, 5471–5479. [PubMed: 20812689]

[35]. Simmons TJ, Lee SH, Park TJ, Hashim DP, Ajayan PM, Linhardt RJ, Carbon 2009, 47, 1561–1564.

[36]. Pasquini LM, Hashmi SM, Sommer TJ, Elimelech M, Zimmerman JB, Environ Sci Technol 2012, 46, 6297–6305. [PubMed: 22515158]

[37]. Aslan S, Deneufchatel M, Hashmi S, Li N, Pfefferle LD, Elimelech M, Pauthe E, Van Tassel PR, J Colloid Interf Sci 2012, 388, 268–273.

[38]. Tiraferri A, Vecitis CD, Elimelech M, Acs Appl Mater Inter 2011, *3*, 2869–2877.

[39]. Rodrigues DF, Elimelech M, Environ Sci Technol 2010, 44, 4583–4589. [PubMed: 20465305]

[40]. Seo Y, Hwang J, Kim J, Jeong Y, Hwang MP, Choi J, Int J Nanomed 2014, 9, 4621–4629.

[41]. Kang S, Mauter MS, Elimelech M, Environ Sci Technol 2008, 42, 7528–7534. [PubMed: 18939597]

[42]. Mutlu GM, Budinger GRS, Green AA, Urich D, Soberanes S, Chiarella SE, Alheid GF, McCrimmon DR, Szleifer I, Hersam MC, Nano Lett 2010, 10, 1664–1670. [PubMed: 20377197]

[43]. Ema M, Gamo M, Honda K, Regul Toxicol Pharm 2016, 74, 42–63.

[44]. Porter D, Sriram K, Wolfarth M, Jefferson A, Schwegler-Berry D, Andrew M, Castranova V, Nanotoxicology 2008, 2, 144–154.

[45]. Sager TM, Porter DW, Robinson VA, Lindsley WG, Schwegler-Berry DE, Castranova V, Nanotoxicology 2007, 1, 118–129.

[46]. Elgrabli D, Abella-Gallart S, Aguerre-Chariol O, Robidel F, Rogerieux F, Boczkowski J, Lacroix G, Nanotoxicology 2007, *1*, 266–278.

[47]. Hu QL, Bai X, Hu GQ, Zuo YY, ACS nano 2017, 11, 6832–6842. [PubMed: 28541666]

[48]. Xu Y, Luo Z, Li SX, Li WG, Zhang XR, Zuo YY, Huang F, Yue TT, Nanoscale 2017, 9, 10193–10204. [PubMed: 28485435]

[49]. Keller S, Berghoff K, Kress H, Sci Rep-Uk 2017, 7.

[50]. Pauwels AM, Trost M, Beyaert R, Hoffmann E, Trends Immunol 2017, 38, 407–422. [PubMed: 28416446]

[51]. Chen T, Nie HY, Gao X, Yang JL, Pu J, Chen ZJ, Cui XX, Wang Y, Wang HF, Jia G, Toxicol Lett 2014, 226, 150–162. [PubMed: 24530353]

[52]. Wang P, Nie X, Wang Y, Li Y, Ge CC, Zhang LL, Wang LM, Bai R, Chen ZY, Zhao YL, Chen CY, Small 2013, 9, 3799–3811. [PubMed: 23650105]

[53]. Zhu JY, Wang J, Hou JW, Zhang YT, Liu JD, Van der Bruggen B, J Mater Chem A 2017, 5, 6776–6793.

[54]. Whitehead KA, Vaidya M, Liauw CM, Brownson DAC, Ramalingam P, Kamieniak J, Rowley-Neale SJ, Tetlow LA, Wilson-Nieuwenhuis JST, Brown D, McBain AJ, Kulandaivel J, Banks CE, Int Biodeter Biodegr 2017, 123, 182–190.

[55]. Lukowiak A, Kedziora A, Strek W, Adv Colloid Interfac 2016, 236, 101–112.

[56]. Li RB, Mansukhani ND, Guiney LM, Ji ZX, Zhao YC, Chang CH, French CT, Miller JF, Hersam MC, Nel AE, Xia T, ACS nano 2016, 10, 10966–10980. [PubMed: 28024366]

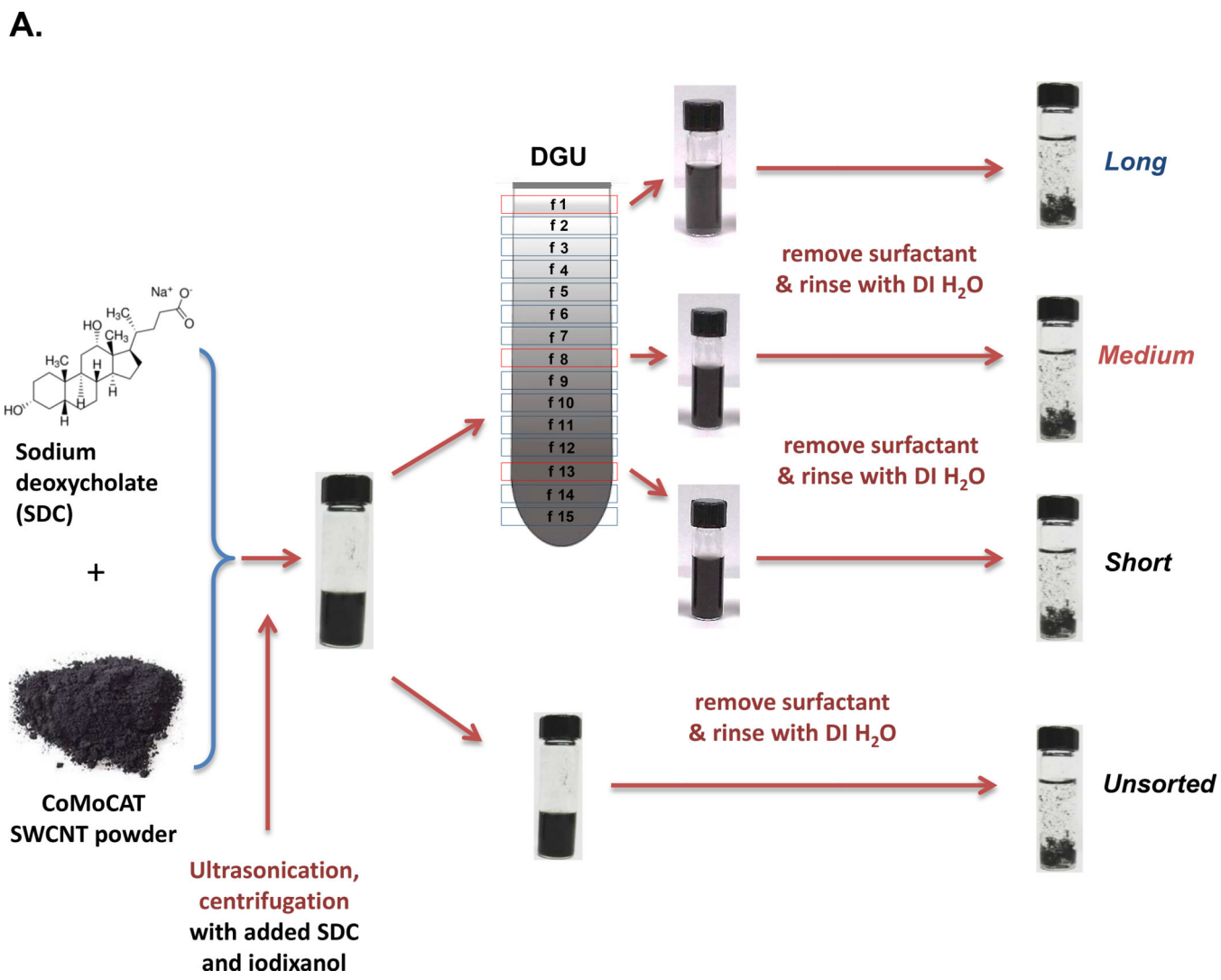

B.

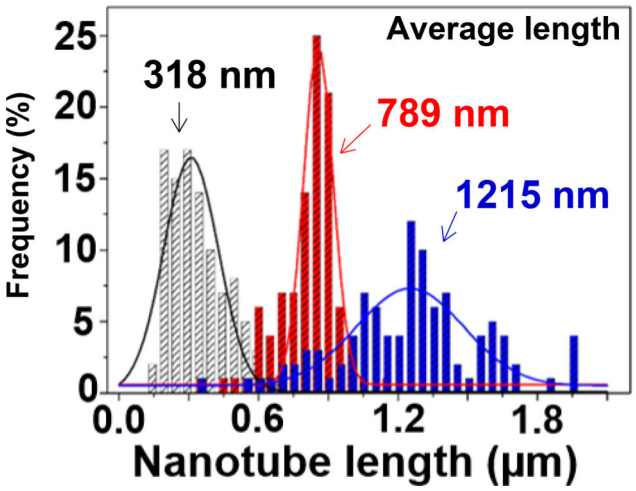

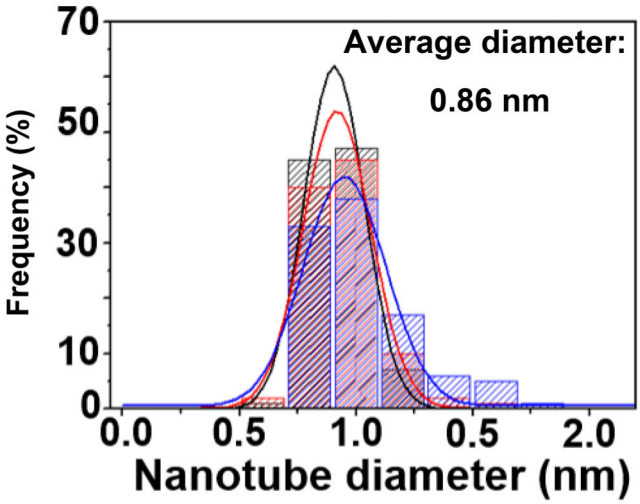

C.

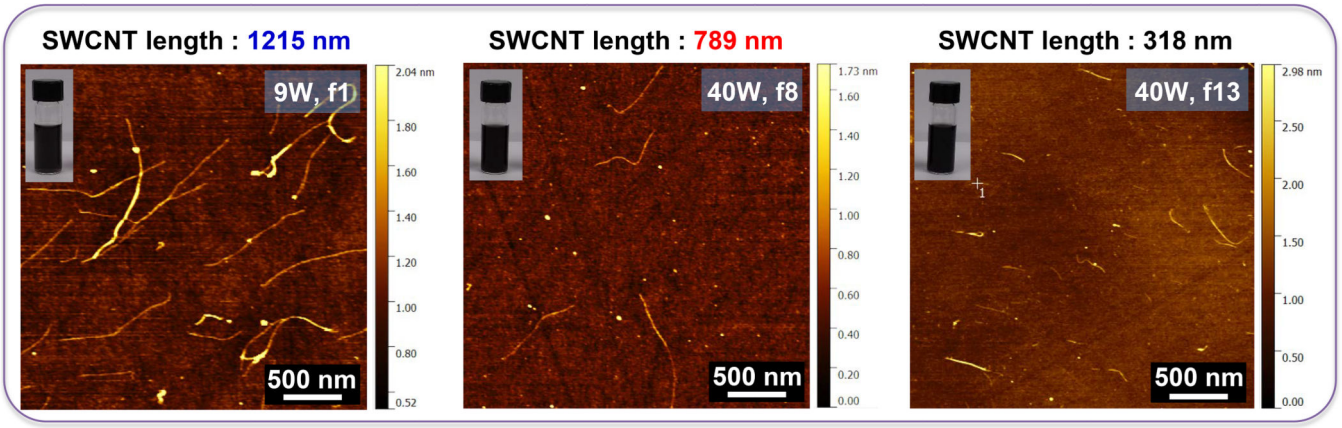

D.

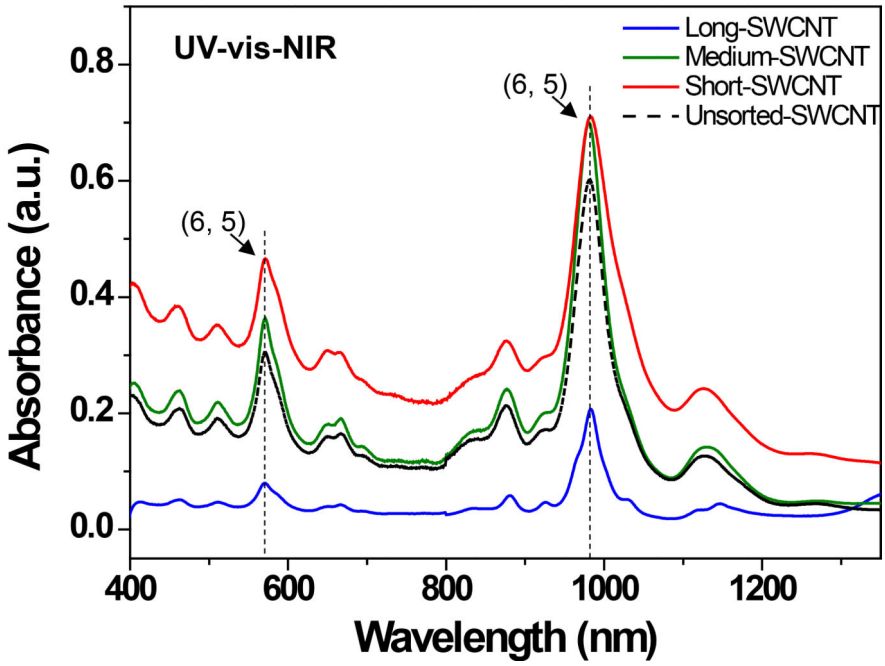

Figure 1: Fractionation and characterization of length-sorted SWCNTs.

(A) Scheme to explain the density gradient ultracentrifugation (DGU) procedure for preparing length-sorted SWCNTs. (B) Length and diameter data were obtained for the sorted tubes through the use of AFM. The average diameter of the of the sorted SWCNTs was 0.86 nm, while the average lengths were measured to be 318 nm, 789 nm and 1215 nm for tube categories labeled as short, medium and long, respectively. Histograms were obtained for at least 100 individual SWCNTs in each case. (C) Representative AFM images of the three length-sorted samples. (D) UV-Vis-NIR absorption spectra of the length-sorted SWCNTs. The two absorption peaks ~566 nm and ~976 nm are characteristic of the semiconducting (6, 5) CoMoCAT SWCNTs used throughout this study.

*f: fraction

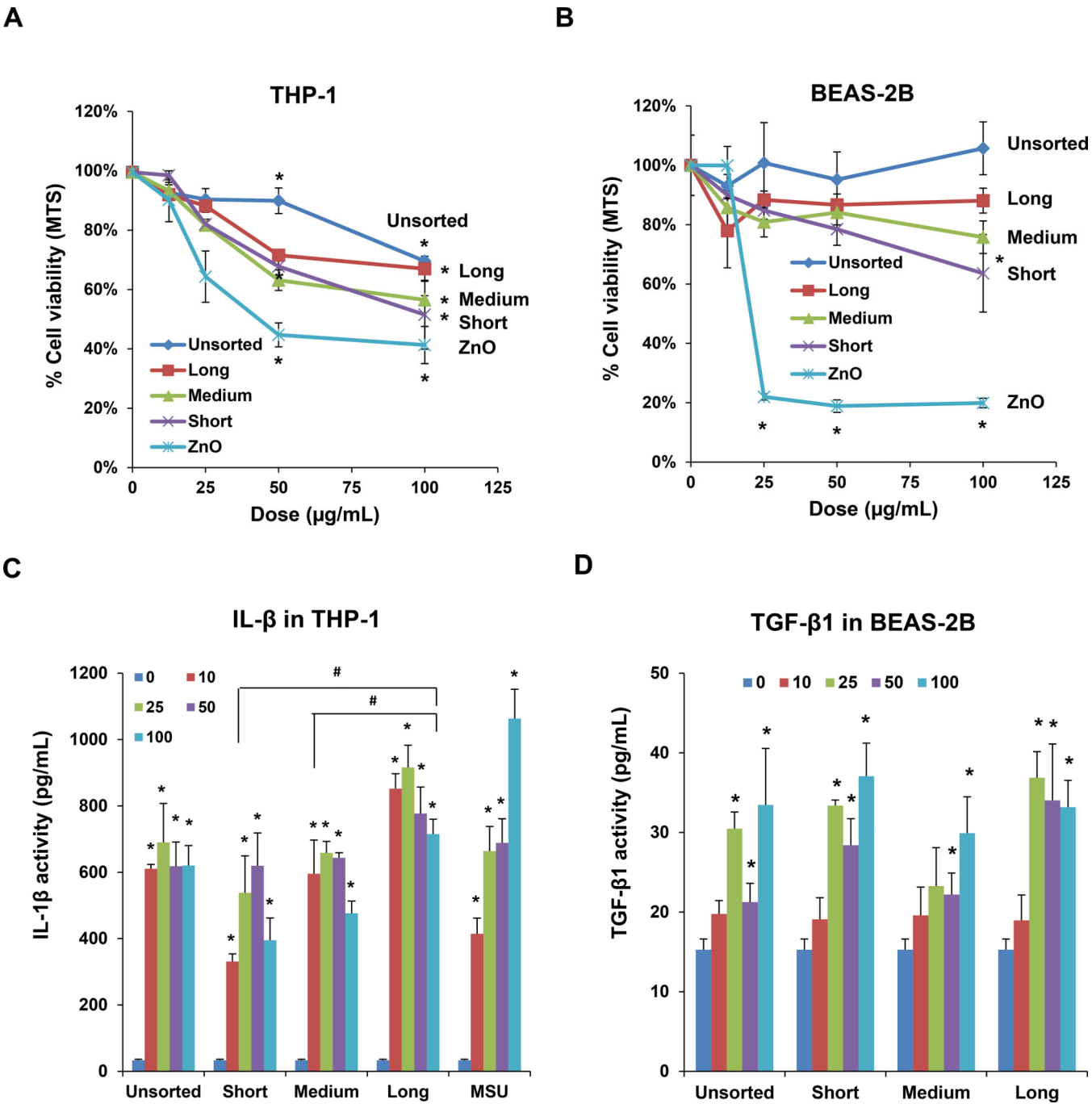

E

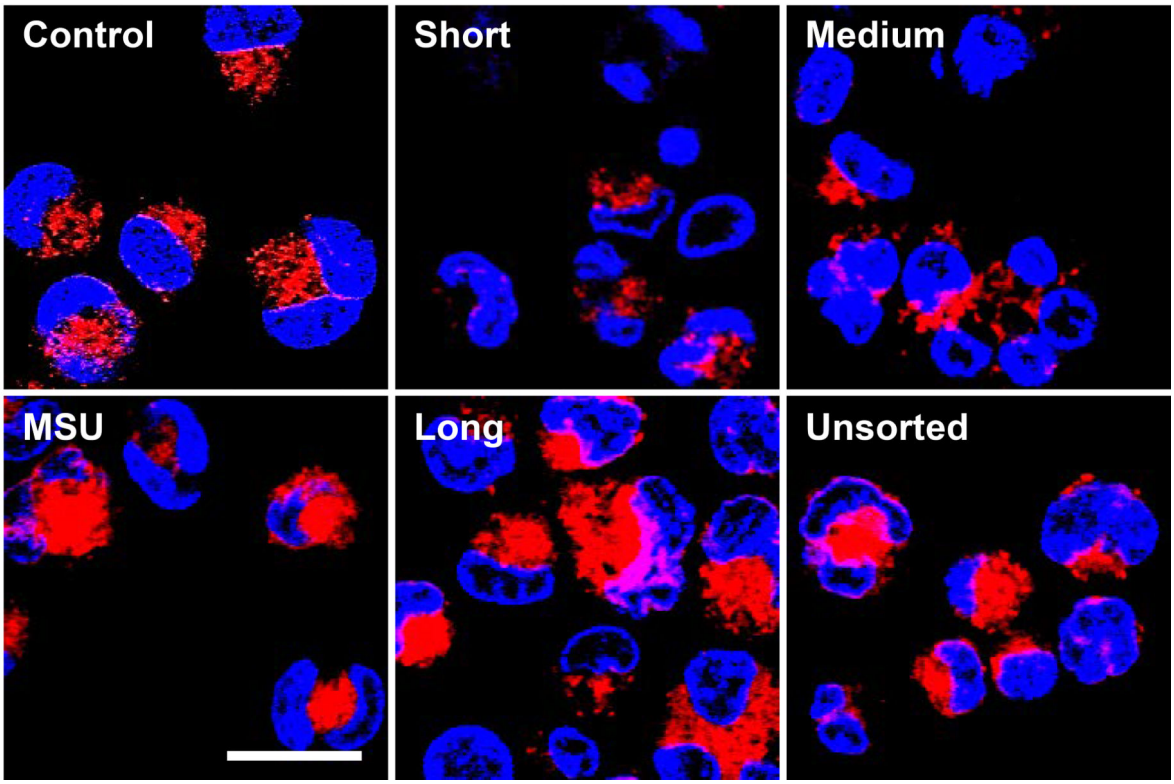

Figure 2: Cytotoxicity and pro-inflammatory cytokine production in THP-1 and BEAS-2B cells exposed to SWCNTs.

The MTS assay was used to assess the cytotoxic effects of SWNCTs in (A) THP-1 and (B) BEAS-2B cells. Both cell types were exposed to 12.5, 25, 50, and 100 μg/mL for each category of sorted and unsorted SWCNTs for 24 h. The media were replaced with the MTS working solution, and following the removal of the supernatants, absorbance was read at 490 nm in a microplate reader (SpectroMax M5e, Molecular Devices, Sunnyvale, CA, USA). All the MTS values were normalized with respect to the non-treated control, which was regarded as representing 100% viability. The supernatants were used to quantify the IL-1β (C) and TGF-β1 (D) levels by ELISA. *$p < 0.05$ compared to control; # $p<0.05$ compared between the two groups indicated for all dose levels respectively. (E) Confocal microscopy demonstrating the lysosomal damage in THP-1 cells by Magic Red staining. THP-1 cells were seeded into 8-well chamber slides and incubated with 100 μg/mL of sorted and unsorted SWNCT suspensions in complete RPMI 1640 for 24 h. After fixation and permeabilization, cells were stained with Magic Red (ImmunoChemistry Technologies) and Hoechst 33342 dye, followed by visualization under a confocal 1P/FCS inverted microscope. Monosodium urate (MSU) crystals were used as a positive control,

demonstrating that the punctate Magic Red staining seen in intact lysosomes (control cells) changes to diffuse cytosolic fluorescence after damage to the lysosomal membrane. The scale bar represents 2 μm in length.

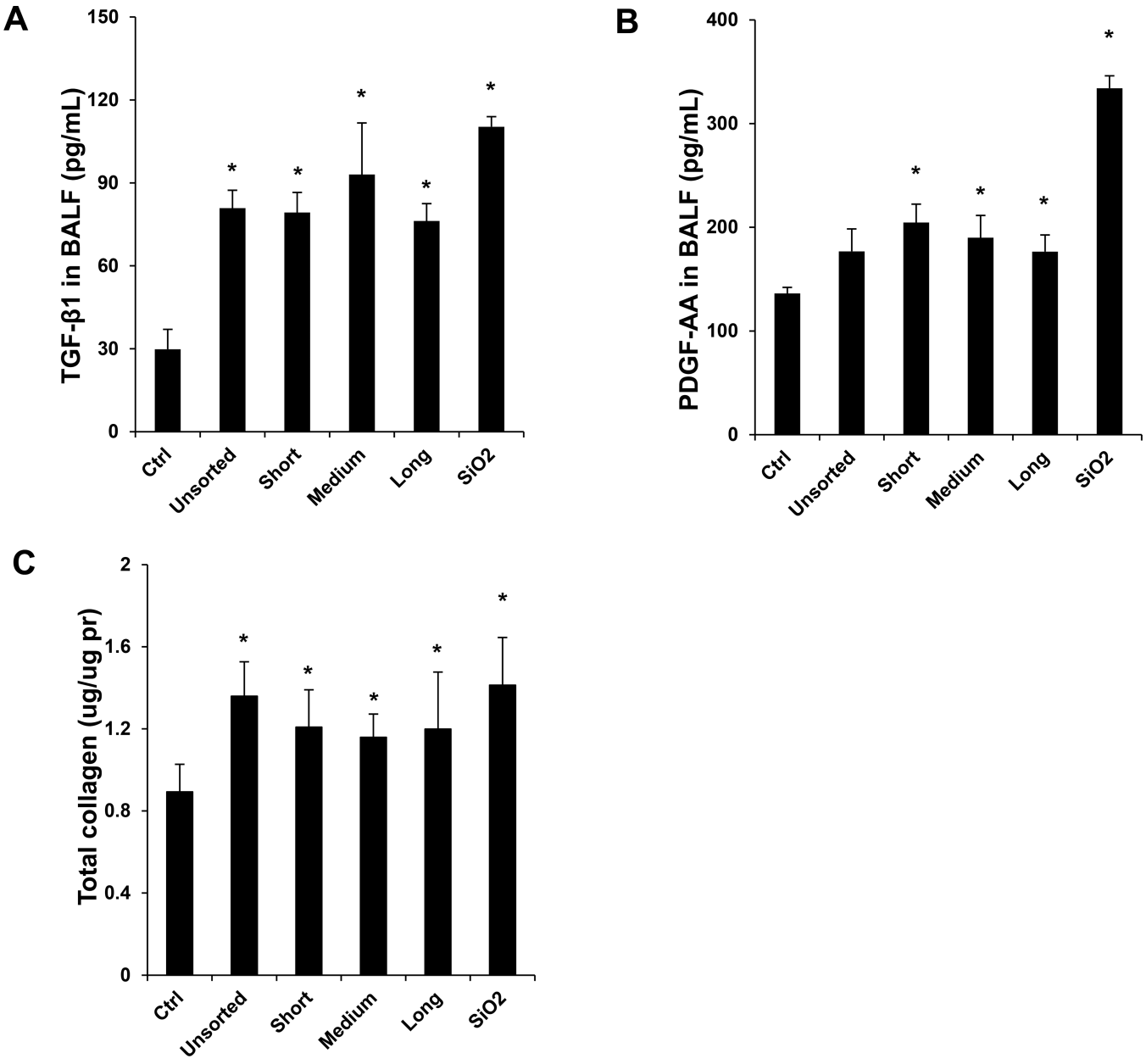

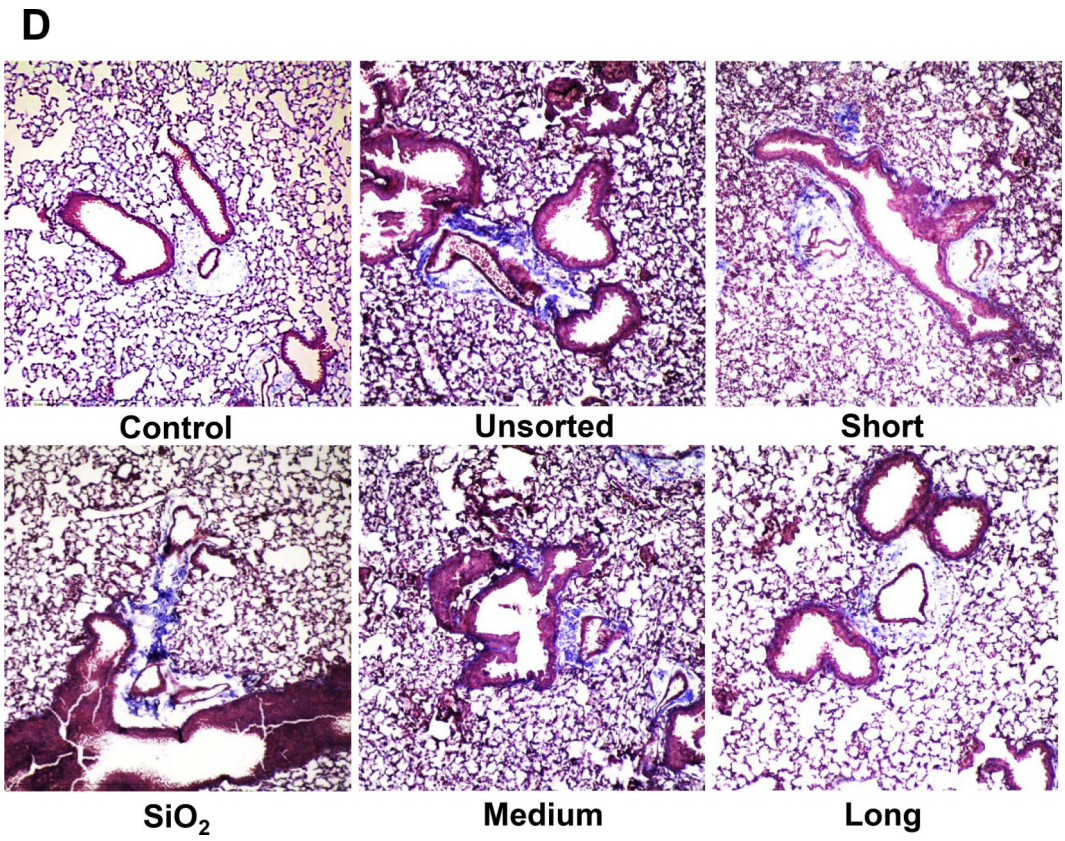

Figure 3: Assessment of the pro-fibrogenic effects of the length-sorted SWNCTs in mice.

C57BL/6 mice were exposed to 2.0 mg/kg bolus doses of SWNCTs delivered by one-time oropharyngeal aspiration. Animals were euthanized after 21 d, and BALF was collected to determine (A) TGF-β1 and (B) PDGF-AA levels. (C) Assessment of total collagen content by a Sircol kit (Biocolor Ltd., Carrickfergus, UK). *$p < 0.05$ compared to control. (D) Collagen deposition in the lung was assessed by staining lung slices with Masson's trichrome. Collagen is stained blue in the images viewed under 100× magnification. Animals exposed to quartz (SiO_2) served as a positive control.

A

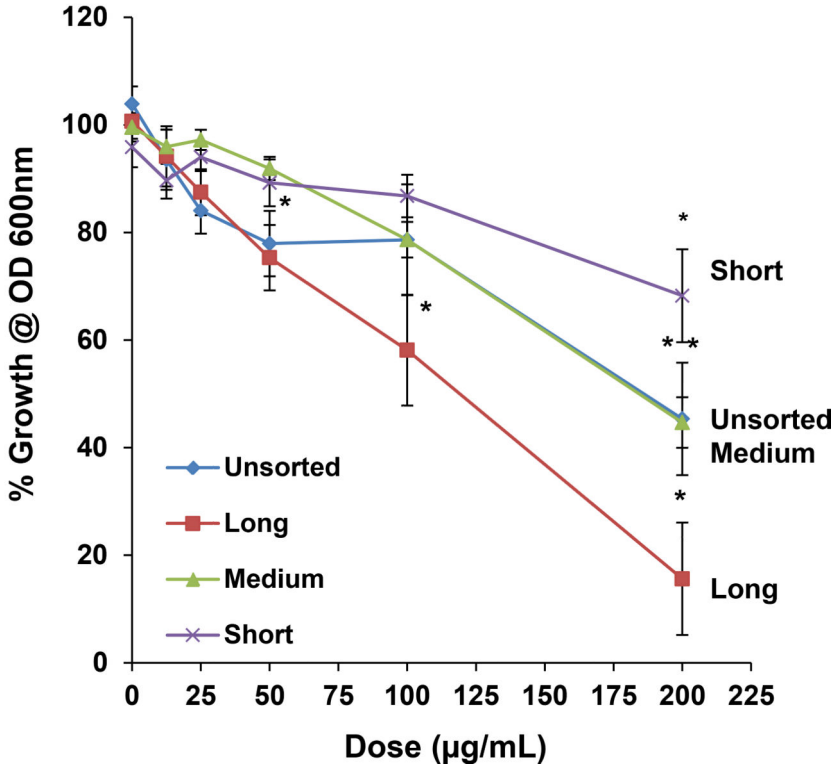

B.

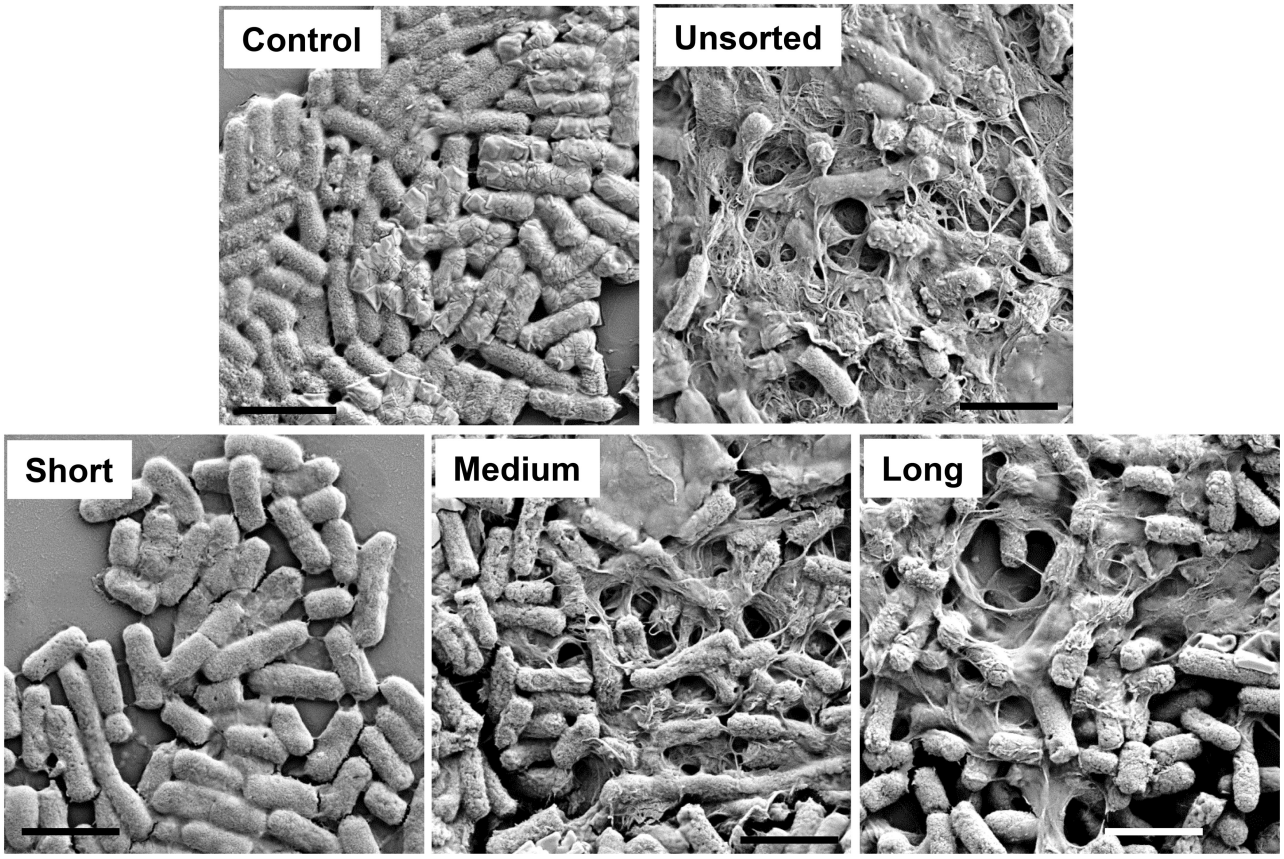

Figure 4: Assessment of the antibacterial effects of length-sorted SWNCTs in E. coli.

(A) E. coli cell growth was assessed by optical absorbance (OD 600 nm) in a plate reader (Spectro Max M5e, Molecular Devices, Sunnyvale, CA, USA). The cultures were incubated with 12.5, 25, 50, 100 and 200 μg/mL SWNCTs for 24 h in regular LB medium. (B) Scanning electron microscopy (SEM) was used to assess morphological changes in E. coli exposed to sorted and unsorted tubes at 200 μg/mL for 24 h. After fixation and dehydration, the cells were imaged under a JEOL JSM-67 field emission scanning electron microscope at 10 kV. The scale bars represent 2 μm in length.

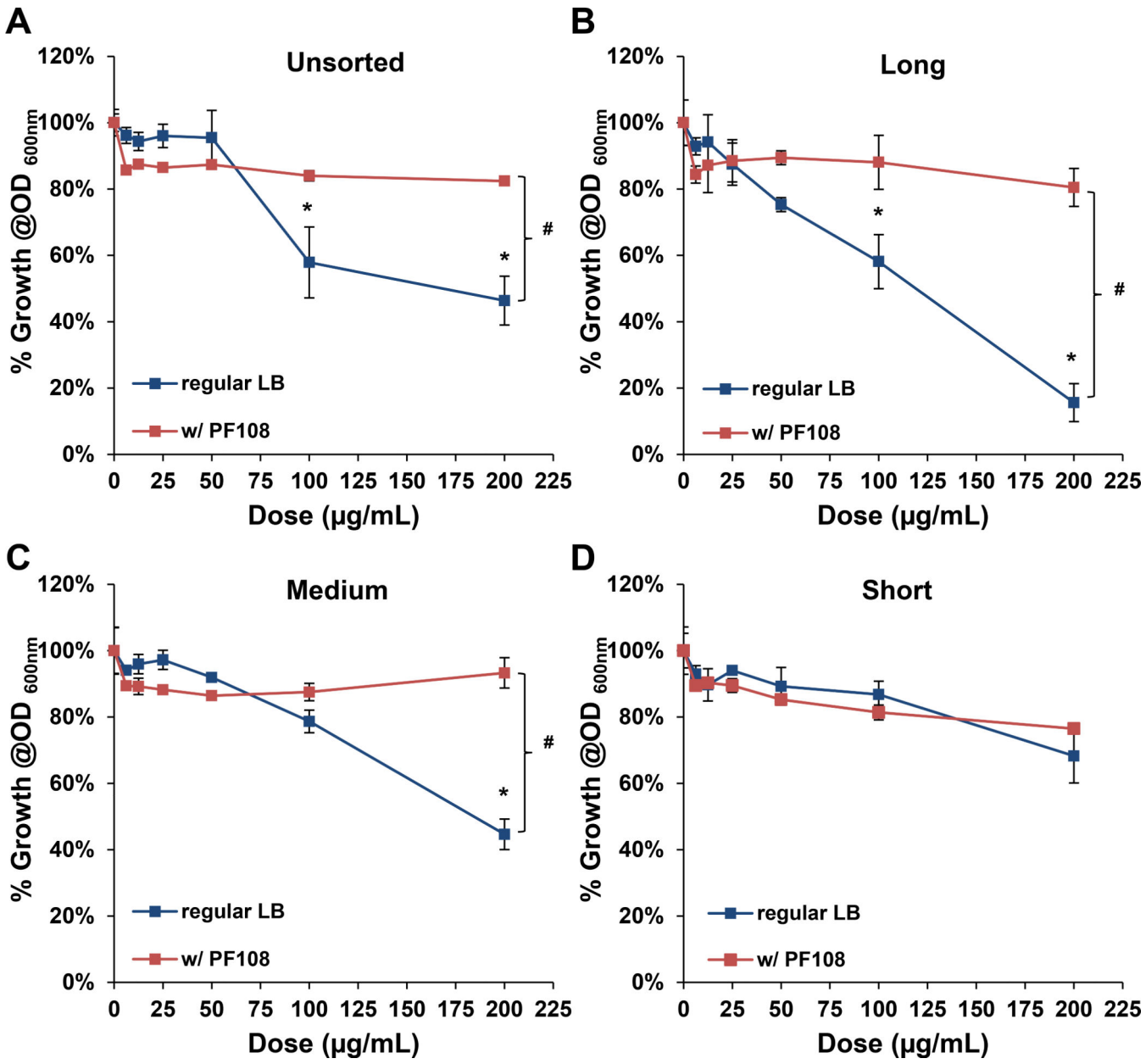

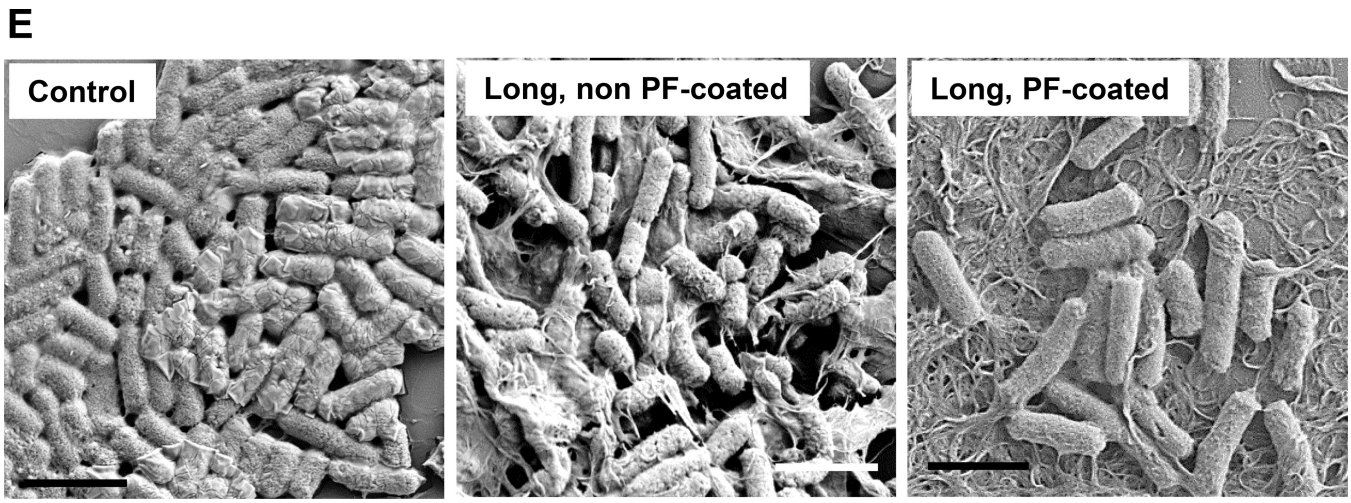

Figure 5: Cellular growth of E. coli after treatment by Pluronic F108 coated SWCNTs.

Cellular growth of E. coli exposed to sorted and unsorted SWCNTs (with or without Pluronic F108 coating was measured at OD 600 nm). Growth inhibitory curves are shown for: (A) unsorted, (B) long, (C) medium and (D) short SWCNTs. *$p < 0.05$ compared to control; # $p<0.05$ during comparison of the two groups indicated. (E). SEM images to show the morphological changes in E. coli, following exposure to long, non PF108-coated and long, PF108-coated SWCNTs. The scale bars represent a length scale of 2 μm.

Table 1.

Metal impurities in Length-sorted SWCNTs.

SWCNT	unsorted	short	medium	long
Co (wt %)	7.80	4.01	0.70	1.55
Mo (wt %)	8.55	5.27	3.76	4.18

Table 2.

Hydrodynamic diameter and zeta potential of SWCNTs.

	SWCNT	DI H2O	RPMI1640	BEGM	LB	LB+glu	LB+PF108
hydrodynamic size (nm)	unsorted	12341±743	1802±47	2335±201	2179±137	1855±132	587±31
	Short	10124±698	1377±623	1645±358	1772±102	1664±119	399±37
	medium	17712±316	1617±337	1763±126	1917±199	1974±154	451±49
	Long	25002±663	1992±639	2306±717	2138±251	2360±187	596±74
ζ potential (mV)	unsorted	−17.3±1.0	−11.7±0.5	−8.3±1.4	−13.3±3.1	−12.6±0.8	−11.1±1.2
	Short	−11.0±0.4	−13.6±0.7	−12.9±0.7	−11.1±0.6	−7.2±0.7	−7.3±0.1
	medium	−16.7±0.2	−7.1±0.1	−6.8±1.0	−13.5±1.4	−9.6±0.9	−6.4±0.9
	Long	−9.9±0.1	−11.4±0.2	−14.6±0.5	−8.6±0.3	−9.8±0.5	−5.6±3.0

The elemental composition was determined by ICP-MS.

The hydrodynamic diameters of SWCNTs in H_2O, BEGM, RPMI1640, LB, LB (supplied with additional glucose) and the hydrodynamic diameters of Pluronic F108 coated SWCNTs in LB were determined through the use of high-throughput dynamic light scattering (HT-DLS, Dynapro Plate Reader, Wyatt Technology). The zeta potential was measured using a Zeta Sizer Nano-ZS (Malvern Instruments, Worcestershire WR, U.K.).